A CONTROL STRATEGY FOR REDUCING THE TORQUE RIPPLE WITH OPTIMAL STATOR FLUX DIRECT TORQUE CONTROLLED INDUCTION MOTOR DRIVE

Rajesh Kumar, R.A. Gupta, Bhangale S.V.
Malaviya National Institute of Technology, JLN Marg, Jaipur, INDIA 302 017
rkumar_mnit@rediffmail.com, rag_mnit@rediffmail.com, bhangale_sv@yahoo.com

Abstract: *Direct Torque Control (DTC) is an emerging technique for controlling the PWM inverter-fed induction motor drives (IMD). It allows the precise and quick control of the IM flux and torque without calling for complex control algorithms. In principle, moreover, DTC requires only the knowledge of the stator resistance. In spite of its simplicity, DTC allows a good torque control in steady state and transient operating conditions to be obtained. If number of possibilities in the vector selection process is greatly increased then this lead to a more accurate control system, which result in a reduction in the torque and flux ripples. A new switching methodology is proposed where each sector of conventional DTC is divided to two half sector (total 12 sector) and a proper vector set is defined for each provides a total 14 vectors. The performance of proposed methodology is investigated, compared, and results are validated through both by simulation and experimentation.*

Key words: *induction motor, direct torque control (DTC) Flux optimization*

1. Introduction

The induction motor is very popular in variable speed drives due to its well known advantages of simple construction, ruggedness, and inexpensive and available at all power ratings. Progress in the field of power electronics and microelectronics enables the application of induction motors for high-performance drives where traditionally only DC motors were applied. Thanks to sophisticate control methods, induction motor drives offer the same control capabilities as high performance four quadrant DC drives. A major revolution in the area of induction motor control was invention of field-oriented control (FOC) or vector control by Blaschke [1] and Hasse [2].

In vector control methods, it is necessary to determine correctly the orientation of the rotor flux vector, lack of which leads to poor response of the drive. The main drawback of FOC scheme is the complexity. The new technique was developed to find out different solutions for the induction motor torque control, reducing the complexity of FOC schemes known as Direct Torque control (DTC).

Direct Torque control (DTC) for induction motor was introduced about more than twenty years ago by Japanese and German researchers Takahashi and Noguchi [3]. DTC was considered as an alternative to the field oriented control scheme to overcome the weakness of scheme. In DTC, the torque and flux are directly controlled by using the selection of optimum voltage vectors. The switching logic control facilitate the generation of the stator voltage space vector, with a suitable choice of the switching pattern of the inverter [4], on the basis of the knowledge of the sector (supplied by the stator flux model block) in which the stator flux lies, and of the amplitudes of the stator flux and the torque. The sector identification depends on the accurate estimation of stator flux position.

However, the generation of only six non-zero voltage vectors by the voltage source inverter is a drawback. The required torque is met for only few switching instants and most of the time the generated voltage vectors produce a torque that is either more or less than the required torque. As a result ripples are generated in the torque as well as flux waveforms. Some techniques like parallel inverter configuration have been proposed to increase number of switching voltage vector [5]-[7]. These schemes are able to reduce the torque ripple but they require more switching devices and capacitor for voltage division.

Direct torque and flux control (DTFC) based space-vector modulation (DTC-SVM) for induction motor sensorless drives was introduced by [8],here improved flux estimator is presented to compensate error related with pure integrator .The direct torque and flux control is implemented as VSC (variable structure controllers), and the SVM is employed to reduce the torque and current ripple and to ensure constant switching frequency by [9], this approach is modified to improve drive performance at low speed operation in [10].

Increase of inverter switching frequency by a space vector modulation scheme is another effort taken for torque ripple reduction it involves several complicated equations. [11]-[13]. These methods achieve some improvements such as torque ripple reduction and fixed switching frequency operation, however, have somehow increased the complexity of the control technique in DTC and diminished the main feature of DTC, which is simple control structure. The 12 sector DTC method presented in [14] for permanent magnet synchronous motor and in [15]-[16] for induction motor are tried to reduce scheme complexity.

This paper is focused on the means of the reducing torque ripple at optimal stator flux. The circular trajectory of the stator flux is divided to twelve sectors and a new switching table is defined. In this switching strategy, some additional vector sets are used so that they prevent

fast jumping of motor torque and it causes the reduction of the torque ripple. A closed loop stator flux estimation algorithm is implemented its leads the improvement in scheme performance. This method has no need to the machine parameters and higher sampling frequency.

In section 2 the basic induction motor model is initially presented and then the fundamentals of basic DTC are explained. The proposed control algorithm is presented in section 3. The simulation results of proposed scheme are to compare basic scheme, finally validated experimentally and presented in section 4.

2. Mathematical Model of Induction Motor and Basic Concept of DTC

A. Mathematical model

The dynamic model of the induction motor is derived by transforming the three phase quantities into two phase direct and quadrature axes quantities. The mathematical model in compact form can be given in the stationary reference frame as fallows [17].

$$\begin{pmatrix} v_{ds} \\ v_{qs} \\ v_{dr} \\ v_{qr} \end{pmatrix} = \begin{pmatrix} R_s + L_s p & 0 & L_m p & 0 \\ 0 & R_s + L_s p & 0 & L_m p \\ L_m p & \omega_r L_m & R_r + L_r p & \omega_r L_r \\ -\omega_r L_m & L_m p & -\omega_r L & R_r + L_r p \end{pmatrix} \times \begin{pmatrix} i_{ds} \\ i_{qs} \\ i_{dr} \\ i_{qr} \end{pmatrix} \quad (1)$$

$$\psi_{ds} = L_s\, i_{ds} + L_r\, i_{dr} \;\;,\;\; \psi_{qs} = L_s\, i_{qs} + L_r\, i_{qr} \quad (2)$$

$$\psi_{dr} = L_r\, i_{dr} + L_s\, i_{ds} \quad \psi_{qr} = L_r\, i_{qr} + L_s\, i_{qs} \quad (3)$$

Where v_{ds}, v_{qs}, i_{ds}, i_{qs} R_s, L_s, R_r, L_r, L_m, Ψ_{ds}, Ψ_{qs}, Ψ_{dr}, Ψ_{qr} and θ_r are the d-q axes voltages and currents, stator resistance, stator inductance, rotor resistance, rotor inductance, mutual inductance between the stator and rotor windings, stator flux linkages, rotor flux linkages and the rotor position respectively.

B. DTC principle review

In order to understand DTC principle some of the equations of the induction motor need to be reviewed. The electromagnetic torque obtained from machine flux linkages and currents is as:

$$T_e = \frac{3}{2}\frac{P}{2} L_m (i_{qs}\psi_{dr} - i_{ds}\psi_{qr}) \quad (4)$$

Where T_e, P, Ψ_{dr}, Ψ_{qr} are the electromagnetic torque, number of poles, rotor d-q axes fluxes respectively.
The electromagnetic torque can be expressed as a function of the stator flux and the rotor flux space vectors as follows

$$T_e = \frac{3}{2}\frac{P}{2}\frac{L_m}{\sigma L_r L_s}|\psi_r||\psi_s|\sin\theta_e \quad (5)$$

Where σ = Leakage coefficient $1 - \left(\frac{L_m^{\,2}}{L_s L_r}\right)$

The angle between the stator and rotor flux linkage space vectors is *θe as* shown in Fig.1.
The stator flux linkage, voltage and torque equations in d-q axis stationary reference frame can be obtained as fallows:

$$v_{ds} = R_s\, i_{ds} + p\psi_{ds} \quad (6)$$

$$v_{qs} = R_s\, i_{qs} + p\psi_{qs} \quad (7)$$

$$\psi_{ds} = \int (v_{ds} - R_s\, i_{ds})dt \quad (8)$$

$$\psi_{qs} = \int (v_{qs} - R_s\, i_{qs})dt \quad (9)$$

$$\psi_s = \sqrt{\psi_{ds}^{\,2} + \psi_{qs}^{\,2}} \quad (10)$$

$$\theta_e = \tan^{-1}\left(\frac{\psi_{qs}}{\psi_{ds}}\right) \quad (11)$$

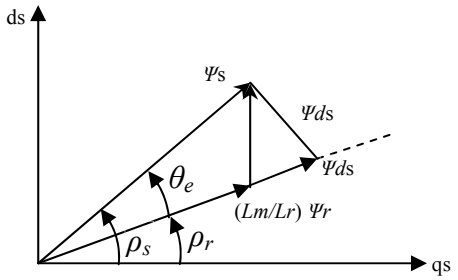

Fig.1 Stator and rotor flux-linkage space vectors.

From equation (5) it is clear that the motor torque can be varied by changing the rotor or stator flux vectors. The rotor time constant of a standard squirrel-cage induction machine is very large, thus the rotor flux linkage changes slowly compared to the stator flux linkage. However, during a short transient, the rotor flux is almost unchanged. Thus rapid changes of the electromagnetic torque can be produced by rotating the stator flux in the required direction, which is determined by the torque command. On the other hand the stator flux can instantaneously be accelerated or decelerated by applying proper stator voltage phasors.

Stator flux can be adjusted by the stator voltage according to the stator voltage equation in stator fixed coordinates (6)-(7).If the voltage drop in the stator resistance is neglected the variation of the stator flux is directly proportional to the stator voltage applied:

$$\vec{v}_s \propto \frac{\mathrm{d}\vec{\psi}_s}{\mathrm{dt}} \quad \text{i.e. } \vec{v}_s \propto \frac{\Delta\vec{\psi}_s}{\Delta \mathrm{t}} \quad (12)$$

This simply means that the tip of the stator flux will follow that of the stator voltage space vector multiplied by the small change in time which will form a circular locus.
Circular locus of the stator flux is divided to six equal sections referred to inverter voltage vectors. For sector first, two adjacent voltage vectors, which give the minimum switching frequency, are selected to increase or

decrease the amplitude of stator flux, respectively. So for each section, a proper voltage vector set is proposed. The proposed voltage vectors are applied to motor so that amplitude of the flux and torque remain with in prescribed band limit. Figure 2 shows proposed DTC scheme where the inverter switching state is determined by the torque and flux comparator error, and instantaneous position of stator flux (11). For basic DTC there are 6 non-zero voltage vectors,v_1(100), v_2(110), v_3(010), v_4(01 1),v_5(001), v_6(101) 60°apart from each other and two zero voltage vectors, v_0 (000) and v_7(111) as shown in figure 3.

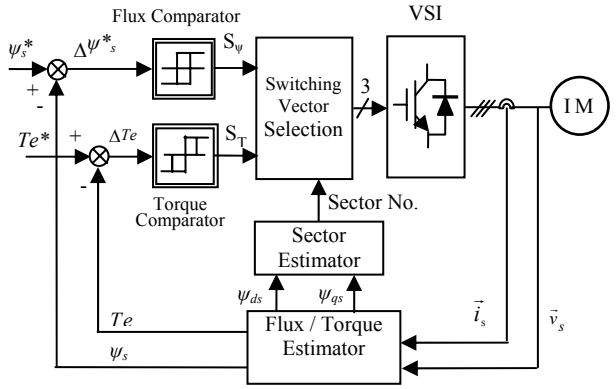

Fig.2 Block diagram of the proposed DTC

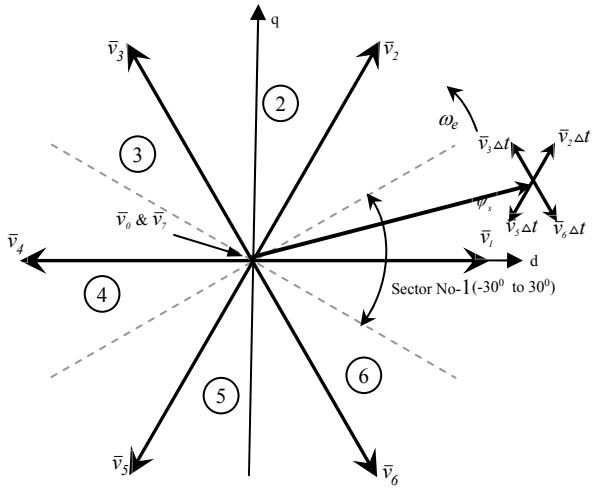

Fig.3 Stator flux vector and the inverter voltage vector movement in the six sector plane.

Table -1 Optimum voltage switching vector look up table for 6 sector plane

Sector Nos.		1	2	3	4	5	6
ψ_s	*Te*						
FI ($\psi_s\uparrow$)	1 (TI)	v_2	v_3	v_4	v_5	v_6	v_1
	0 (TC)	v_7	v_0	v_7	v_0	v_7	v_0
	-1(TD)	v_6	v_1	v_2	v_3	v_4	v_5
FD ($\psi_s\downarrow$)	1 (TI)	v_3	v_4	v_5	v_6	v_1	v_2
	0 (TC)	v_7	v_0	v_7	v_0	v_7	v_0
	-1(TD)	v_5	v_6	v_1	v_2	v_3	v_4

FI- flux increased, FD-Flux decreased, TI-Torque increased TD-Torque decreased, TC-Torque constant.

The suitable voltage vector is selected from the optimum switching table-1 that is depending on the position of the stator flux (11), flux and torque error. So it is possible to control both flux and torque independently by applying a suitable voltage vectors to the motor.

3 New DTC Control Strategy

A Switching scheme

In the conventional switching increase in torque obtained by the alternate selection of the two forward vectors (i.e.v_2 & v_3 for sector 1). At the beginning of sector stator flux vector and voltage vector v_2 are nearly orthogonal. If v_2 is applied to the motor the flux vector rotate fast cause increased in angle between the stator and rotor flux. From the torque equation (5) the machine torque increased but which results in more torque ripple in the beginning of sector.

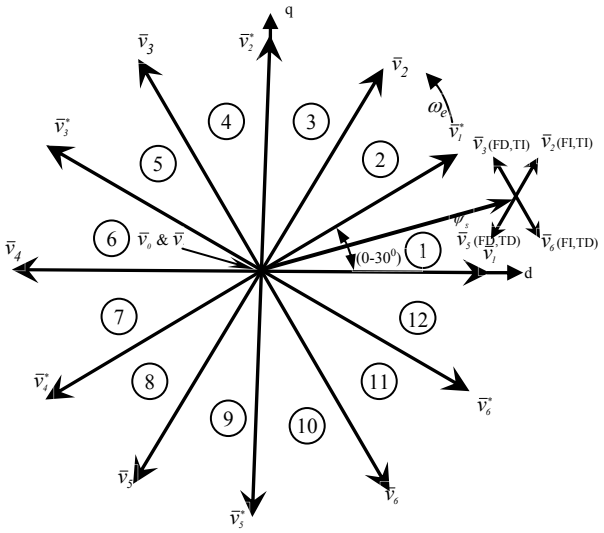

Fig.4 Stator flux vector and the inverter voltage vector movement in the twelve sector plane.

Table-2 Optimum voltage switching vector look up table for 12 sector plane

ψ_s	FI			FD		
Te	TI	TC	TD	TI	TC	TD
Sec-1	v^*_2	v_7	v_6	v_3	v_0	v^*_5
Sec-2	v_3	v_0	v^*_1	v^*_4	v_7	v_6
Sec-3	v^*_3	v_0	v_1	v_4	v_7	v^*_6
Sec-4	v_4	v_7	v^*_2	v^*_5	v_0	v_1
Sec-5	v^*_4	v_7	v_2	v_5	v_0	v^*_1
Sec-6	v_5	v_0	v^*_3	v^*_6	v_7	v_2
Sec-7	$^*v_5$	v_0	v_3	v_6	v_7	v^*_2
Sec-8	v_6	v_7	v^*_4	v^*_1	v_0	v_3
Sec-9	v^*_6	v_7	v_4	v_1	v_0	v^*_3
Sec-10	v_1	v_0	v^*_5	v^*_2	v_7	v_4
Sec-11	v^*_1	v_0	v_5	v_2	v_7	v^*_4
Sec-12	v_2	v_7	v^*_6	v^*_3	v_0	v_5

To overcome this problem a new switching concept has been proposed with the optimal flux algorithm. The concept is that if the locus of the stator flux is divided into twelve equal sectors instead of six sectors each of 30 degrees. As shown in Fig.4. there are, fourteen switching combinations can be selected in a voltage source inverter, out of which twelve are nonzero voltage vectors and two zero voltage vectors. The switching states are selected by the position of the synchronous angle (θe), and the results of torque and flux comparators same as in basic DTC. Thus a suitable voltage vector is selected according to the flux and torque demands from the switching table-2 generated for twelve sector method.

B. Stator Flux Optimization

The decrease in torque during the switching state depends upon the stator flux magnitude (command flux) and the switching frequency of operation. To minimize the torque ripple, decrease in torque during inactive state must be kept to its minimum. This requires optimization of the command flux which can be made a function of the command torque. The command flux is chosen to be just large enough to generate the required command torque. This can be achieved by the following optimization.

The stator flux relation for the induction machine is obtained from its mathematical model as:

$$\psi_s = L_s i_s + L_m i_r \tag{13}$$

Where L_s is the stator inductance, L_m, is the magnetizing inductance, i_r the rotor current and i_s the stator current of the machine .The stator flux is also given by:

$$\psi_s = L_s i_m \tag{14}$$

where i_m, is magnetizing current

Then torque relation can be obtained as:

$$T_e = L_s i_m i_r \sin\theta \tag{15}$$

where θ is the angle between the stator current i_s and rotor current i_r

The rotor current ir, is given by [18]

$$i_r = \frac{L_s}{(L_s/L_m)^2 L_d} i_m \cos\theta \tag{16}$$

$$L_d = \frac{L_s L_r - L_m^2}{L_s}$$

From (15) and (16) we have

$$T_e = \frac{L_s^2 i_m^2}{(L_s/L_m)^2 L_d} \cos\theta \sin\theta \tag{17}$$

Substituting equation (13)

$$T_e = \frac{\psi_s^2}{(L_s/L_m)^2 L_d} \sin(2\theta) \tag{18}$$

In order to minimize the stator flux and make it just large enough to generate the command flux we can find the maximum command torque for (18). Torque is maximum when sin(2θ) =1. Thus for θ =45^0 we have

$$T_e^* = \frac{\psi_s^{*2}}{2(L_s/L_m)^2 L_d} \tag{19}$$

Thus the optimized command stator flux ψ_s* for the given command torque T^*_e is obtained by equation (20) bellow:

$$\psi_s^* = \sqrt{2T_e^* (L_s/L_m)^2 L_d} \tag{20}$$

The optimal flux is used in the proposed control scheme to improve the drive performance.

C. Stator Flux Estimation algorithm

In (8) and (9), pure integrators are applied to estimate the stator flux. Notably, initial value error and dc-offset problems exist herein. To improve these problems, solution proposed to use the low-pass filter that has the input–output relation given by a newly proposed integration algorithm is used [19], the Simulink model is developed for stator flux estimation algorithm as shown in Fig.5.

The input output relation of the low pass filter is given by

$$y = \frac{1}{s + \omega_c} x \tag{21}$$

By choosing a low value of cut off frequency (ω_c=10 rad/sec) leads to a better integration, but higher dc bias. A higher value of cutoff frequency ω_c changes the integration output. The d-q axis stator fluxes in the stationary reference frame are mainly computed by the integration of back emf in the d-q frame which can be obtained by the abc to d-q transformation. The stator flux amplitude and angle is calculated from (10) and (11), the absolute value of flux is dc bias signal obtained from the flux limiter block output. These signals are transferred in to original form by using the Polar to Cartesian .This algorithm is suitable for the constant flux operation.

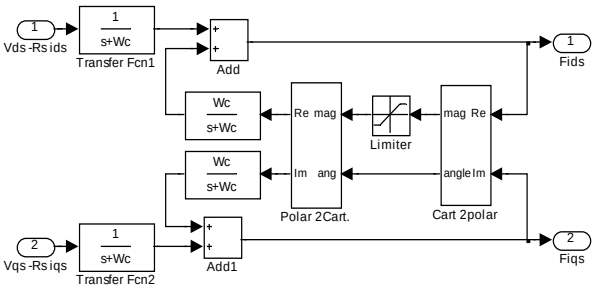

Fig.5 Simulink model of integration method for stator flux estimation

The use of an LP filter in place of a pure integrator reduces the performance of the drive because of the phase and magnitude errors inherent in the LP filter as compared to the pure integrator, particularly at lower frequencies. This drawback overcome by implementation of a phase and magnitude compensation for the voltage-model-based stator flux estimator with LP filter [20]. Comparative analysis of different flux estimator algorithms developed ac motor drive was presented in [21]. Stator flux establishment is depends on the voltage drop on the stator resistance at high speeds, this voltage drop can be ignored. However, at low speeds, this drop tends to be comparable with the input stator voltage results low torque development it creates difficulty in controller operation at low speeds [22].The proposed

stator flux compensator for wide speed range is shown in Fig.6. The speed error is used an input to proportional integral derivative (PID) controller to compensate the stator flux. The torque error, stator flux error and flux angle are the input to the switching table.

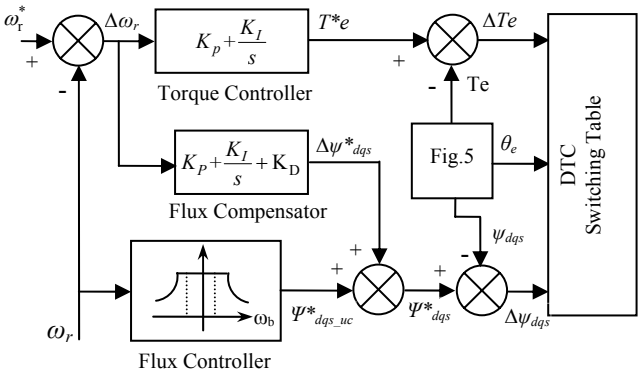

Fig.6 stator flux compensation for DTC scheme.

4. Simulation and Experimental Results

The results of simulation obtained in this work are for the induction motor of 3 HP and parameters as given in appendix. The machine model is implemented for basic DTC scheme and proposed twelve sector switching strategy with stator flux optimization DTC scheme using Matlab /Simulink. To demonstrate the performance of the proposed scheme, some simulations from the proposed scheme are compared with those from the conventional control scheme. First the performance of basic and proposed scheme is checked for speed of 100 rad/sec and the simulation results are obtained under the steady state and transient conditions which are shown in Fig.8 (a) - Fig.8 (d) and Fig.9 (a) -Fig.9 (d). Both schemes basic and modified DTC are applied to the induction motor to check the performance under no load and then switch to speed reversal, which is applied at 0.2 sec. instant. Fig.8 (b) and Fig.9 (b) shows that the steady state torque responses while Fig.8 (d) and Fig.9 (d) shows transient response of torque during the speed reversal. We can observe that the both DTC schemes demonstrate is very good dynamic response but the basic DTC having more ripple than the modified DTC. The torque ripples in modified DTC is reduced remarkably compared with basic DTC nearly more than 35% has been seen in Fig.9 (b) and Fig. 9(d). Fig.8 (a) and Fig.9 (a) shows d-q axis stator currents for both control scheme under no load conditions, after comparing this it is observed that the harmonic distortion is more in basic DTC than modified DTC scheme. Fig.10 (g) and Fig.11 (g) shows the switching sector identification.

The performance of the both scheme is checked for the low speed and high speed (i.e. in flux weakening region) range. The induction motor is run at a speed of 0.3 rad/sec (i.e. ≈3 rpm) under no load up to 15 sec and then a step load torque of 10 N-m is applied. Fig.10 (a)-Fig.10(c) and Fig.11 (a)-Fig.11 (c) shows the scheme performance under low speed operation for basic and modified DTC. The machine is run above the rated speed (i.e.157 rad/sec rotor speed) for the similar load conditions in above case (i.e. first at no load and then switch to step load torque of 10 N-m.). The responses of stator currents, torque and the speed under this operation for both schemes are shown in Fig.10 (d)-Fig.10 (f) and Fig.11 (d)-Fig. 11(f).

For comparison purposes, the harmonic current analysis is performed at the same average switching frequency of 1000 Hz and the fundamental current frequency of 50 Hz. The harmonic analysis is carried for no load and load duration under low and high speed operation and results are shown in Fig- 12(a) , Fig.13 (a) and Fig. 12 (b), Fig. 13 (b). Comparative harmonic analysis results for various speed for no-load and load operation has been depicted in Table 3.

In order to make the experimental validation of the effectiveness of the proposed DTC scheme for torque ripple reduction, a DSP-based induction motor drive system has been built and the result are taken at 100 rad/sec speed.. The experimental setup includes a fully digital controlled IGBT based 5KVA Semikron make PWM voltage source inverter and a 2.2-kW, 415-V, 50-Hz, four-pole squirrel cage induction motor coupled with dc generator which is shown in Fig.7. Basic and proposed DTC schemes have been implemented on dSPACE controller board DS-1104 which consist a DSP processor MPC8240 of 250 MHz. The dSPACE has 4 multiplexed channel, 16-bit sample and hold ADC, 4 parallel channels, 12-bit sample and hold ADC and 8 channel of digital to analog converter (DAC), with 16-bit resolution. The induction motor has the same parameters applied in simulation. The machine currents i_a and i_b sensed by LEM LA 55-P current sensor and voltage sensor LEM LV 100-1000V used to sense the dc bus voltage these signals were interfaced into the controller through an analog to digital converter (A/D) which is separate peripheral unit of controller board. The sampling time set to 0.0001 sec and DSP board was controlled with a PC. Fig 13 (a) - Fig 13 (c) shows response of stator flux, torque and stator currents for basic DTC. The response of modified DTC is depicted in Fig 14 (a) for the d-q axis stator fluxes reflect the reduction in ripples and confirm the effectiveness of flux ripple reduction to decrease the torque ripple as shown in Fig. 14 (b). Fig.14 (c) shows stator currents response under speed reversal for modified DTC.

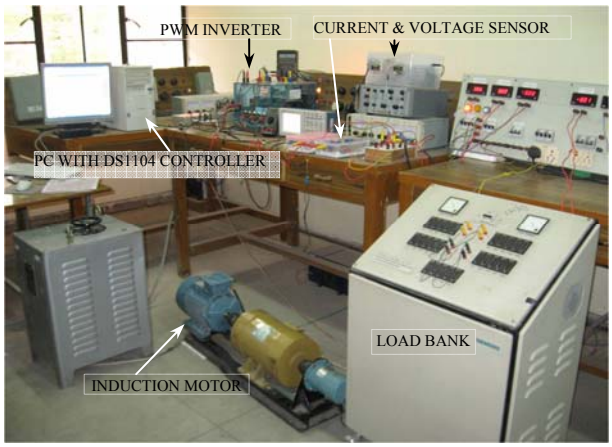

Fig.7 Photo of Experimental setup

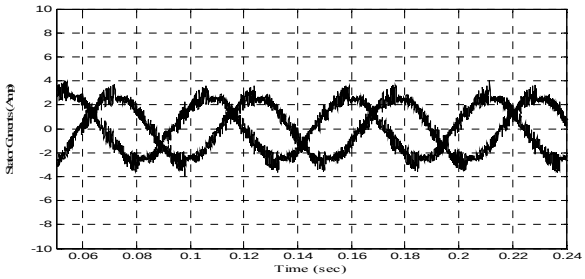

Fig.8 (a) Steady state response d-q axis stator currents for basic DTC (at 100 rad/sec)

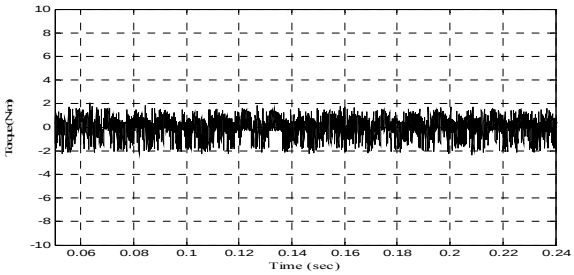

Fig.8 (b) Torque response under the steady state condition for Basic DTC (at 100 rad/sec)

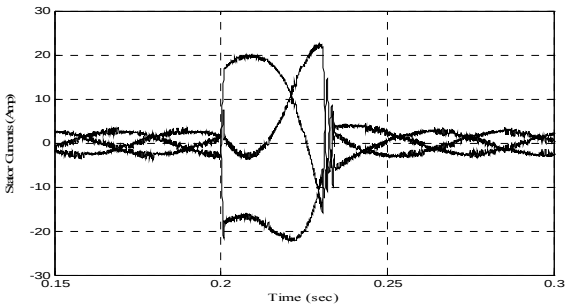

Fig.8 (c) Transient response (speed reversal) of stator currents for basic DTC (at 100 rad/sec)

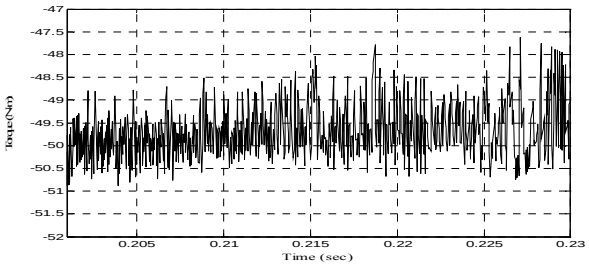

Fig.8 (d) Torque response under the transient condition (during speed reversal) for basic DTC scheme (at 100 rad/sec).

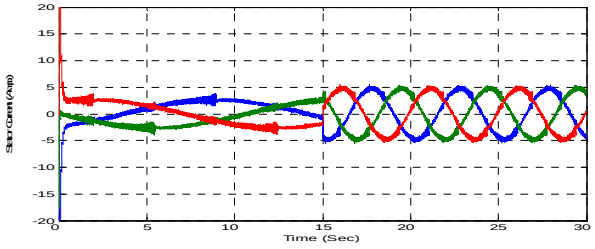

Fig.10 (a) Stator current response at low speed operation for basic DTC

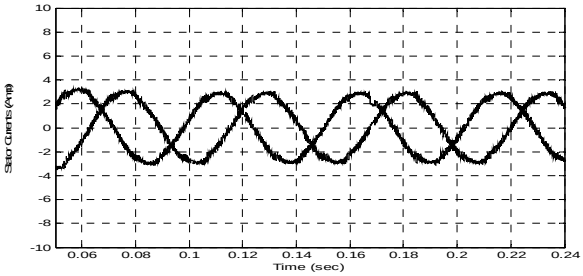

Fig.9 (a) Steady state response d-q axis for stator currents Modified (12 Sector) DTC (at 100 rad/sec)

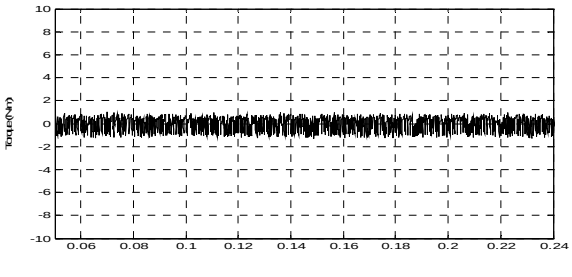

Fig.9 (b) Torque response under the steady state condition for 12 Sector DTC (at 100 rad/sec)

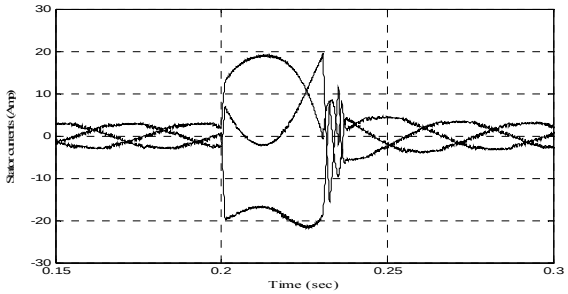

Fig.9 (c) Transient response (speed reversal) of stator currents for 12 Sector DTC (at 100 rad/sec)

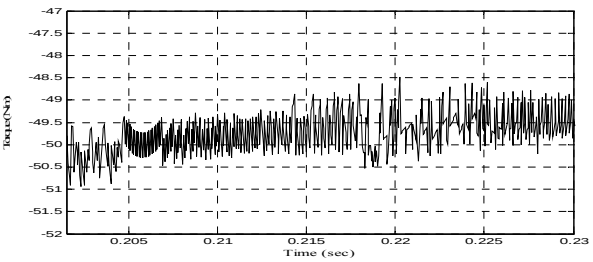

Fig.9 (d) Torque response under the transient condition (during speed reversal) for12_ Sector DTC scheme (at 100 rad/sec).

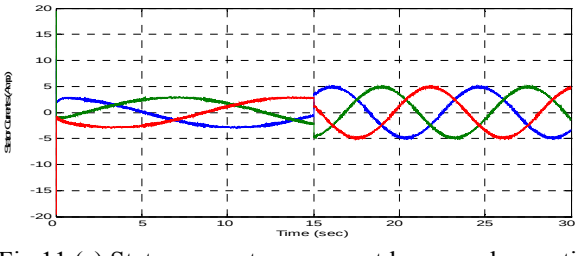

Fig.11 (a) Stator current response at low speed operation for Modified (12 Sector) DTC

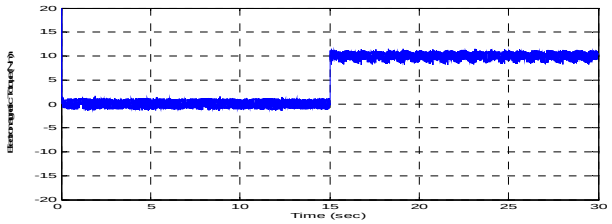

Fig.10 (b) Torque response under the low speed operation for Basic DTC

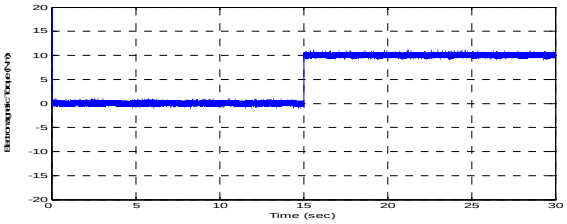

Fig.11 (b) Torque response under the low speed operation for Modified (12 Sector) DTC

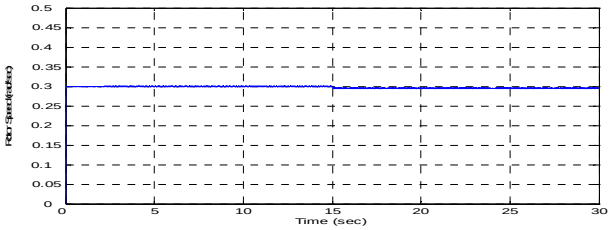

Fig.10 (c) Rotor speed response for basic DTC

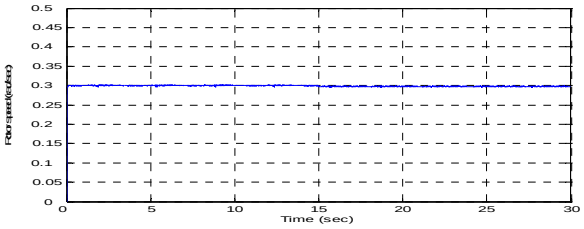

Fig.11 (c) Rotor speed response for Modified (12 Sector) DTC

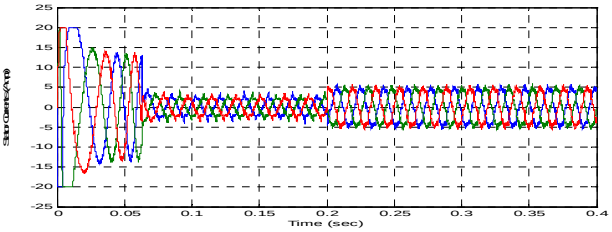

Fig.10 (d) Stator current response under above rated speed for basic DTC

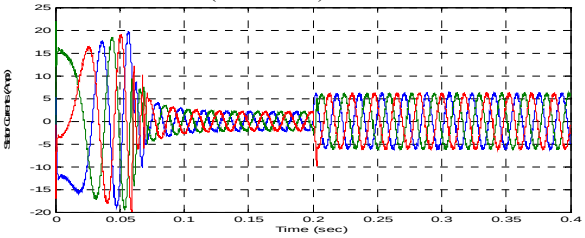

Fig.11 (d) Stator current response under above rated speed for Modified (12 Sector) DTC

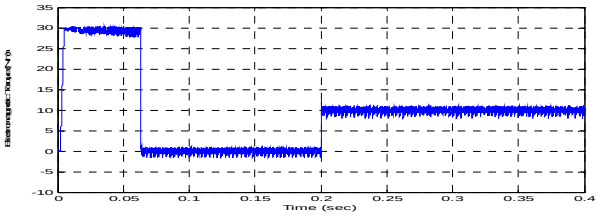

Fig.10 (e) Torque response under above rated speed for basic DTC

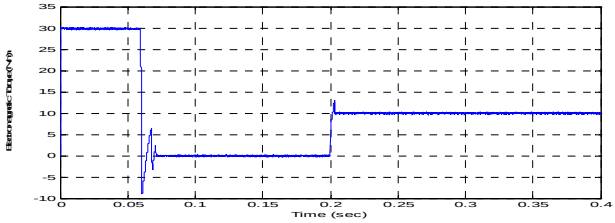

Fig.11 (e) Torque response under above rated speed for Modified (12 Sector) DTC

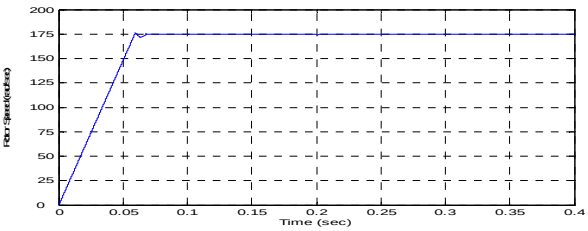

Fig.10 (f) Rotor speed response for basic DTC

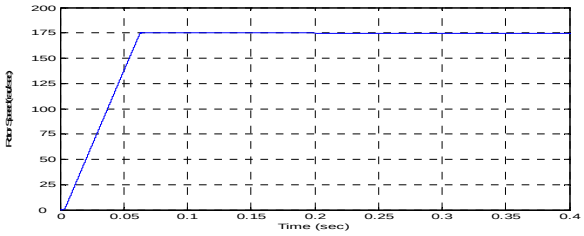

Fig.11 (f) Rotor speed response for Modified (12 Sector) DTC

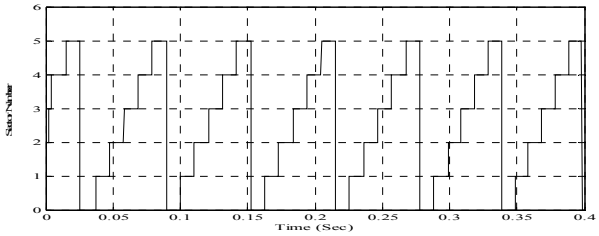

Fig.10 (g) Switching sectors of Basic_ DTC

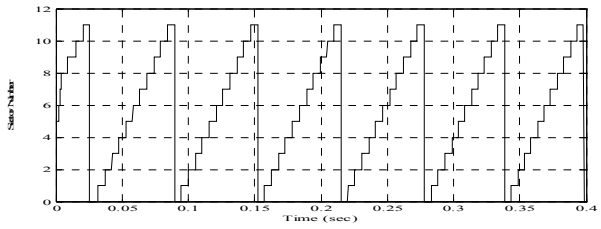

Fig.11 (g) Switching sectors of Modified (12 Sector) DTC

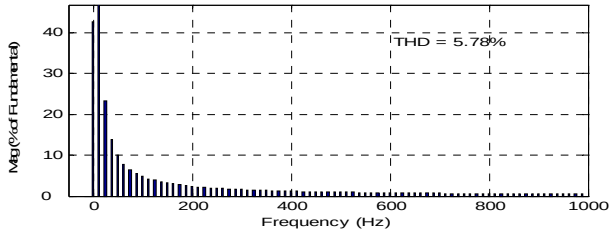

(a)

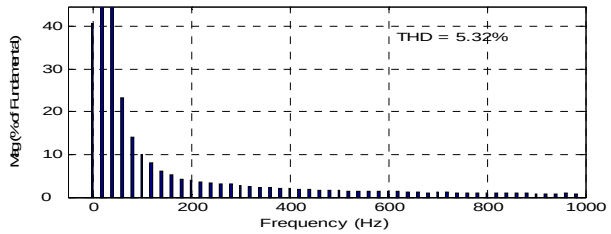

(b)

Fig. 12 (a)Harmonic spectrum of stator current (under no load condition) at low speed (a) and above rated speed (b) for basic DTC

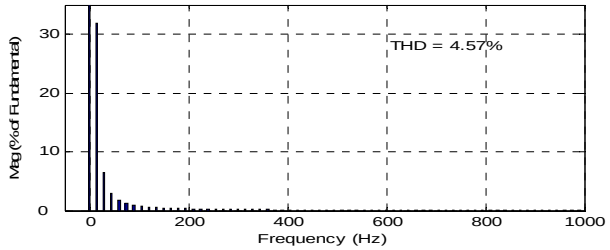

(a)

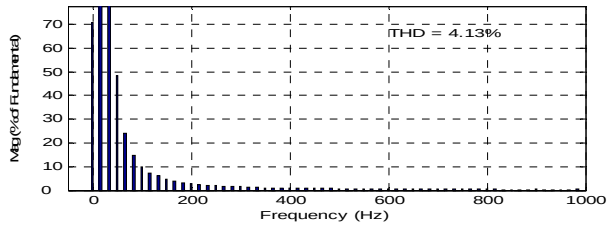

(b)

Fig. 12 (b) Harmonic spectrum of stator current (under load condition) at low speed (a) and above rated speed (b) for basic DTC

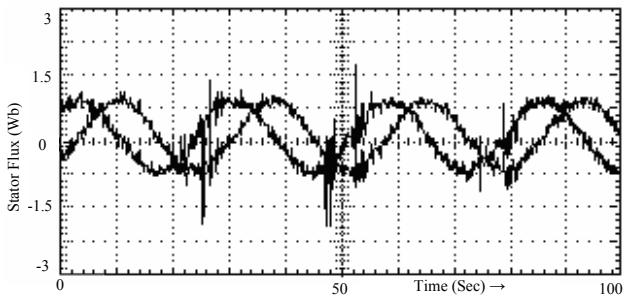

Fig.14 (a) Experimental response of d –q axis stator flux for basic DTC

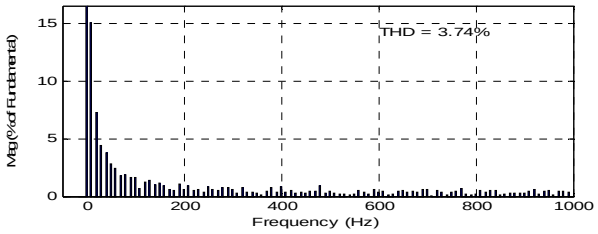

(a)

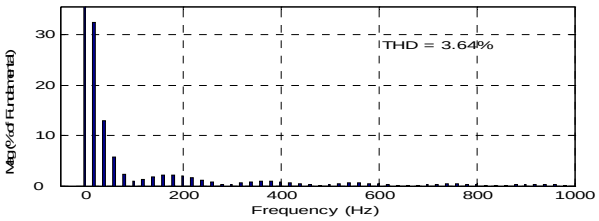

(b)

Fig. 13 (a) Harmonic spectrum of stator current (under no load condition) at low speed (a) and above rated speed (b) for modified DTC

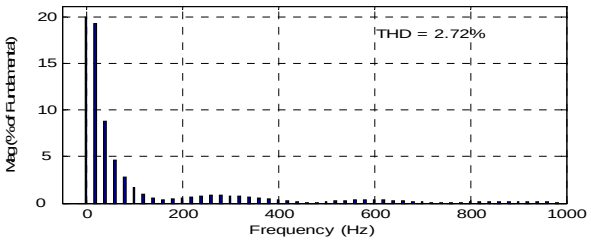

(a)

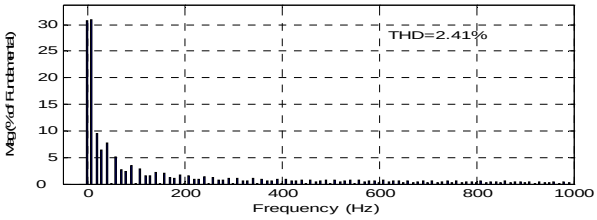

(b)

Fig. 13 (b) Harmonic spectrum of stator current (under load condition) at low speed (a) and above rated speed (b) for modified DT

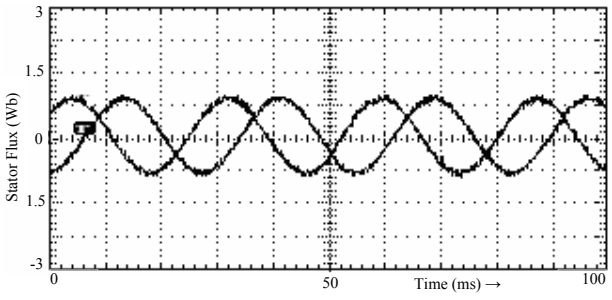

Fig.15 (a) Experimental response of d–q axis stator flux for Modified (12_ Sector) DTC

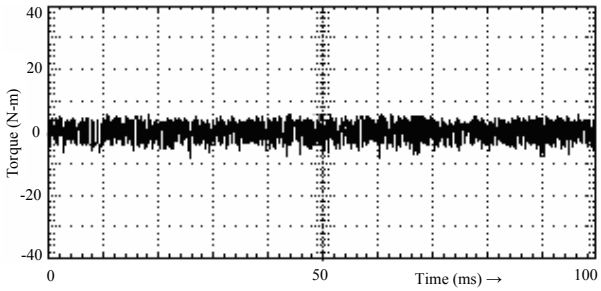

Fig. 14 (b) Experimental response of electromagnetic Torque (basic DTC) under steady state

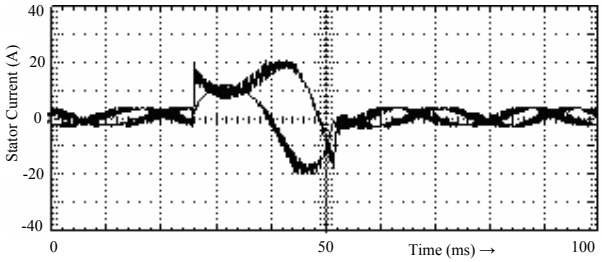

Fig. 14 (c) Experimental response of stator currents (i_{ab}) for basic DTC under transient condition (speed reversal).

Control Scheme	Rotor Speed (rad/sec)	THD (%) of Stator current (A)	
		No load	load
Basic DTC (6-Sector)	Low Speed	5.78%	4.57%
	Above rated speed	5.32%	4.13%
Modified DTC (12-Sector)	Low Speed	3.74%	2.72%
	Above rated speed	3.64%	2.41%

Table 3. Comparison of Total Harmonic Distortion for the basic DTC and modified DTC schemes at various speed for no load and load condition.

5. Conclusions

In this paper the twelve sector switching strategy with flux optimization has been proposed for DTC of voltage source inverter fed induction motor drive. The proposed scheme performance is compared with the basic DTC scheme under the steady state and transient conditions. The simulation and implementation of the DTC drive with the proposed scheme has been presented. Immunity to offset drift is achieved by appropriate closed loop flux estimators. From the simulation and experimental results, it is shown that despite of their simple control structure and implementation, the proposed DTC scheme have managed to significantly reduce the torque and flux ripples

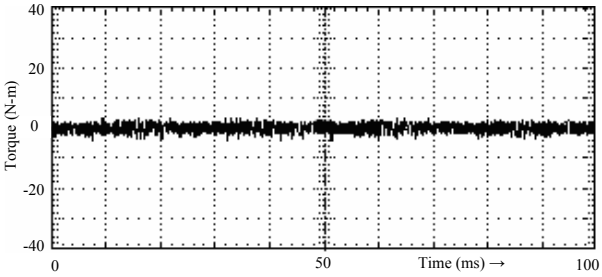

Fig.15 (b) Experimental response of electromagnetic Torque Modified (12_ Sector) DTC under steady state

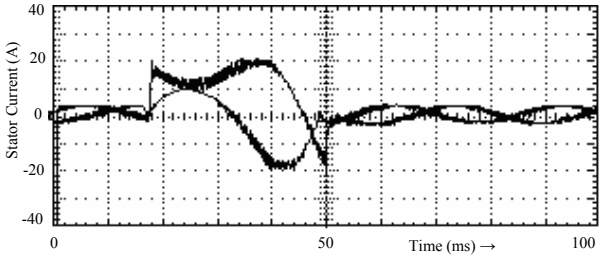

Fig.15 (c) Experimental response of stator currents (i_{ab}) for Modified(12_ Sector) DTC under transient condition (speed reversal)

APPENDIX

The parameters of the three-phase Induction Motor, employed for simulation purpose, in SI units are

2.2 KW (3.0HP) 3 phase 415V, 50 Hz, 1415 rpm, R_s = 10.13 Ω, R_r =13.17 Ω, L_{ls} = 40.165mH, L_{lr}= 40.165mH, L_m = 921.15mH, P = 4, J = 0.02 Kg/m^2, B = 1e-5

References

1. F**.** Blaschke, "The principle of field orientation as applied to the new transvector closed-loop control system for rotating-field machines," *Siemens Rev.,* 1972**.**
2. K**.** Hasse, "Zum Dynamischen Verhalten der Asynchron-machine bei Betriek Mit Variabler Standerfrequenz und Standerspannung," *ETZ-A* , Bd. 9**,** p. 77, 1968.
3. Takahashi and T. Noguchi, "A new quick-response and high efficiency control strategy of an induction machine," *IEEE Trans. Ind. Application.*, vol. 22, pp. 820–827, Sep./Oct. 1986.
4. I.Takahashi and Y. Ohmori, "High-performance direct torque control of an induction motor," *IEEE Trans. Ind. Application.*, vol. 25, pp. 257– 264, Mar./Apr. 1989.
5. Takahashi, I., Ohmori, Y. "High-performance direct torque control of an induction motor," , *IEEE Trans. on Ind. App.* vol. 25, no. 2, pp. 257 – 264, March/April 1989.
6. B. S. Naceri, F. Betta, A. Laggoune, L. "Speed sensorless DTC of induction motor based on an improved adaptive flux observer," *IEEE*

International Conference on Industrial Technology, (ICIT 2005.), pp. 1192 – 1197, Dec. 2005.

7. Brando, G., Rizzo, R. "An optimized algorithm for torque oscillation reduction in DTC-induction motor drives using 3-level NPC inverter," *IEEE Ind. Electronics, International Symposium* vol. 2, pp.1215–1220, 2004.
8. Lascu, C. I. Boldea,, and F. Blaabjerg, "A modified direct torque control for induction motor sensorless drive," *IEEE Transactions on Ind. Applicat.* vol. 36 , no.1, pp. 122 – 130, Jan/Feb. 2000.
9. C. Lascu, I. Boldea, and F. Blaabjerg "Variable-Structure Direct Torque Control-A Class of Fast and Robust Controllers for Induction Machine Drives," *IEEE Transactions on Ind. Electro.* vol.51, no.4, pp. 785 –792, Aug. 2004.
10. C. Lascu, I. Boldea, and F. Blaabjerg "Very-Low-Speed Variable-Structure Control of Sensorless Induction Machine Drives Without Signal Injection," *IEEE Transactions on Ind. Applicat.* vol. 41 , no.2, pp. 591– 598, March/April 2005.
11. Casadei, D. Serra, G. Tani, K. "Implementation of a direct control algorithm for induction motors based on discrete space vector modulation", *IEEE Trans. on Power Electronics,* vol. 15, no. 4, pp. 769 – 777, July 2000.
12. Lascu, C., Boldea, I., Blaabjerg, F. "A modified direct torque control for induction motor sensorless drive" *IEEE Trans. on Ind. App.* vol. 36, no. 1, pp.122 – 130, Jan.-Feb. 2000.
13. Lascu, C., Boldea, I., Blaabjerg, F. "Variable-structure direct torque control - a class of fast and robust controllers for induction machine drives," *IEEE Trans. on Ind. Electronics,* vol. 51, no. 4, pp. 785 - 792, Aug. 2004.
14. L. Bao-hua, L. Wei-guo, Z. Xi-wei, Li Rong; "Research on Direct Torque Control of Permanent Magnet Synchronous Motor Based on Optimized State Selector" IEEE International Symposium on Industrial Electronic, vol. 3, pp. 2105 – 2109, July 2006.
15. R. A. Gupta , Rajesh Kumar, B. Suresh, "Direct Torque control Induction Motor Drive with reduced torque ripple" *IEEE Int. Conf. on Ind. Tech.* ICIT (2006), pp. 2073,2078, Dec 2006.
16. B. Suresh , R. A. Gupta and Rajesh Kumar "12-Sector Methodology of Torque Ripple Reduction in a Direct Torque Controlled Induction Motor Drive" SICE-ICASE International Joint Conference 2006 pp. 3587-3592 Oct. 18-21, 2006.
17. C. M. Ong, *Dynamic Simulation of Electric Machinery* Using Matlab/Simulink, Prentice Hall, 1997
18. P. Vas "Vector control of AC machines *press Oxford 1990.*
19. Jun Hu and Bin Wu "New Integration Algorithms for Estimating Motor Flux over a Wide Speed Range" *IEEE Trans. on power Electro*. vol.13. no 5. pp. 969-977 Sept. 1998.
20. N.R.N. Idris, and A. H. M. Yatim "An Improved Stator Flux Estimation in Steady-State Operation for Direct Torque Control of Induction Machines" *IEEE Tran. on Industry Application,* vol. 38, no. 1, pp. 110-116, Jan/Feb 2002
21. A. W. F. V. Silveira, D. A. Andrade, C. A. Bissochi, T. S. Tavares, L. C. Gomes "A Comparative Study Between Tree Philosophies of Stator Flux Estimation for Induction Motor Drive," *IEEE International Conference Electric Machines & Drives,* vol. 2, pp.1171 – 1176, May 2007.
22. K.K. Shyu, , L.J. Shang, H.Z. Chen, and K.W. Jwo "Flux Compensated Direct Torque Control of Induction Motor Drives for Low Speed Operation, " *IEEE Trans. on Power Electro*. vol. 19, no. 6, pp.1608-1613, Nov 2004.